Multiphoton detachment of H^-. II. Intensity-dependent photodetachment rates and threshold behavior—complex-scaling generalized pseudospectral method

Jingyan Wang and Shih-I Chu
Department of Chemistry, University of Kansas, Lawrence, Kansas

Cecil Laughlin
Department of Mathematics, Nottingham University, Nottingham, England
(Received 3 March 1994)

We extend our previous perturbative study of the multiphoton detachment of H^- [Phys. Rev. A **48**, 4654 (1993)] to stronger fields by considering the intensity-dependent photodetachment rates and threshold behavior. An accurate one-electron model potential, which reproduces exactly the known H^- binding energy and the low-energy e-H($1s$) elastic-scattering phase shifts, is employed. A computational technique, the complex-scaling generalized pseudospectral method, is developed for accurate and efficient treatment of the time-independent non-Hermitian Floquet Hamiltonian $\hat{H}_F$. The method is simple to implement, does not require the computation of potential matrix elements, and is computationally more efficient than the traditional basis-set-expansion–variational method. We present detailed nonperturbative results of the intensity- and frequency-dependent complex quasienergies $(E_R, -\Gamma/2)$, the complex eigenvalues of $\hat{H}_F$, providing directly the ac Stark shifts and multiphoton detachment rates of H^-. The laser intensity considered ranges from 1 to 40 GW/cm^2 and the laser frequency covers 0.20–0.42 eV (in the c.m. frame). Finally we perform a simulation of intensity-averaged multiphoton detachment rates by considering the experimental conditions of the laser and H^- beams. The results (without any free parameters) are in good agreement with experimental data, both in absolute magnitude and in the threshold behavior.

PACS number(s): 32.80.Rm, 32.80.Fb, 42.50.Hz

I. INTRODUCTION

There is currently much interest in the study of multiphoton detachment of H^- both experimentally [1–3] and theoretically [4]. The H^- ion, one of the simplest yet important three-body atomic systems, possesses only one bound state. Structures in the continuum far above the ionization threshold can be safely ignored for moderate laser fields. Thus, multiphoton detachment from the ground state to the continua can be studied without interference from any doubly excited intermediate electronic states and resonances. These simplifying features render the multiphoton detachment of H^- a unique and fundamental process to study.

Theoretical study of multiphoton detachment of H^-, however, is by no means straightforward. In fact, wide discrepancies exist between many of the earlier predictions, even for two- and three-photon (weak-field) detachment cross sections which have occupied most of the theoretical efforts so far. Since Geltman [4] has already provided a comprehensive review of previous theoretical works in this field, we shall not elaborate here.

In a recent study of multiphoton detachment of H^- [5] (hereafter we refer to it as paper I), we have constructed an accurate one-electron model, which reproduces precisely the known H^- binding energy [6] and the low-energy e-H($1s$) elastic-scattering phase shifts [7]. Generalized cross sections, based on lowest-nonvanishing-order perturbation theory, are evaluated by an accurate and efficient algorithm for the solution of the associated set of inhomogeneous differential equations [8]. One- to eight-photon detachment cross sections σ_n $(n=1,2,\ldots,8)$ are determined. Our one-photon photoabsorption cross sections are in excellent agreement with earlier accurate correlated two-electron calculations [9]. Our σ_2 and σ_3 are in reasonable good agreement with recent two-electron *ab initio* calculations [10]. Overall, it appears that this recent study [5] provides the consistent results with the accuracy for higher-order σ_n $(n>3)$ comparable to that of lower orders $(n=2,3)$. Detailed discussion of this previous work is given in Ref. [5].

The motivations of this paper are threefold.

(i) First we extend the study of multiphoton detachment of H^- to the *nonperturbative* regime. Both the experimental [3] and theoretical works [4,5] indicated that the process of multiphoton detachment of H^- under the experimental conditions of Ref. [3] cannot be described adequately by perturbation theory. Intensity-dependent threshold shifts and photodetachment rates must be considered. To study such "strong" field phenomena, we shall extend the non-Hermitian Floquet formalism [11,12], allowing direct nonperturbative determination of the intensity-dependent complex quasienergy $(E_R, -\Gamma/2)$ associated with the decaying ground state. The real part (E_R) provides the ac Stark shift and the imaginary part $(\Gamma/2)$ is related to the multiphoton detachment rate.

(ii) Second we introduce a computational technique, the complex-scaling generalized pseudospectral (CSGPS) method, for accurate and efficient determination of the

complex quasienergies of H^- associated with the non-Hermitian Floquet Hamiltonian. As will be demonstrated in later sections, the CSGPS method does not require the computation of the potential matrix elements and is computationally simpler and faster than the conventional basis-set-expansion—variational method. Further, the CSGPS method is computationally much more efficient and accurate than some other grid discretization methods (such as finite difference). Thus, the CSGPS method appears to be capable of providing a powerful general numerical technique for the treatment of atomic and molecular resonances.

(iii) Third we determine the intensity-averaged photodetachment rates of H^- by a simulation of the experimental conditions of the H^- and laser beams.

We begin in Sec. II the discussion of the generalized pseudospectral discretization method and its extension to the studies of the bound-state eigenvalue problem, the resonance-state complex eigenvalue problem, and the complex quasienergy resonances within the non-Hermitian Floquet formalism. We also introduce a mapping procedure for removing the Coulomb singularity to facilitate the pseudospectral discretization. In Sec. III we present our one-electron model of H^-. The justification of its accuracy has been described in paper I [5]. In Sec IV we present our detailed nonperturbative results of the intensity- and frequency-dependent complex quasienergies, providing multiphoton detachment rates of H^- as well as ac Stark shifts of the ground state. The laser intensity considered ranges from 1 to 40 GW/cm^2 and the laser frequency covers 0.20–0.42 eV. In Sec. V we perform a simulation of intensity-averaged multiphoton detachment rates by considering the experimental conditions of the laser and H^- beams. Good agreement with the experimental data is achieved. This is followed by a conclusion in Sec. VI.

II. COMPLEX-SCALING GENERALIZED PSEUDOSPECTRAL METHOD: NEW APPROACH FOR THE SOLUTION OF MULTIPHOTON QUASIENERGY RESONANCES

In this section we describe a new approach, the complex-scaling generalized pseudospectral method, for accurate and efficient treatment of atomic and molecular resonances, including multiphoton quasienergy resonances (within the non-Hermitian Floquet Hamiltonian formalism) [11,12]. The method does not require the computation of potential matrix elements (which is usually the most time-consuming part of atomic and molecular structure calculations using the conventional basis-set-expansion–variational method), is simple to implement, and provides the values of the wave functions directly at the space grid points. As will be shown later, the generalized pseudospectral methods are far more efficient and accurate than the finite-difference method and computationally more efficient and advantageous than the basis-set-expansion–variational method. The generalized pseudospectral method is a natural extension of the generalized Fourier-grid Hamiltonian (GFGH) methods recently developed for the studies of atomic and molecular bound and resonance states [13–15]. The GFGH methods employ Fourier series and require the mesh points to be equally spaced. The generalized pseudospectral methods employ orthogonal polynomials (such as Legendre or Chebyshev polynomial) and allow for uneven mesh spacing. It has been shown recently that the GFGH methods [13–15] work well for potentials without singularity, such as the Morse potential for chemical bond, etc. However, for problems involving singularity and/or long-range potentials (such as the Coulomb potential), the generalized pseudospectral method with appropriate mapping (see Sec. II C) is the more effective approach.

While the pseudospectral method has been extensively studied in mathematics [16] in the past decade and applied to fluid dynamics [17] (such as aerodynamics, meteorology, and oceanology), little attention, however, has been paid to the usefulness of the method (at least in its most updated form) in the study of atomic and molecular structure and resonances [18]. As such, we discuss below the essence of the pseudospectral method and its several generalizations for the treatment of atomic and molecular bound and resonance states, as well as complex quasienergy resonances.

A. Bound-state eigenvalue problems

The central part of the pseudospectral method is to approximate the exact solution $\phi(x)$ by order N or $N+1$ polynomial $\phi_N(x)$:

$$\phi(x)\simeq\phi_N(x)=\sum_{l=0}^{N} a_l u_l(x) , \tag{1}$$

where $u_l(x)$'s are orthogonal polynomials satisfying

$$\int_a^b w(x)u_l(x)u_{l'}(x)dx=a_l\delta_{ll'} , \tag{2}$$

$w(x)$ is the weighing factor, and α_l is the normalization constant. The pseudospectral method further requires that the approximation be exact, i.e., $\phi_N(x_j)=\phi(x_j)$, at the collocation points x_j (to be described below). The expansion coefficients a_l can be written as

$$\begin{aligned} a_l&=\frac{1}{\alpha_l}\int_a^b w(x)\phi(x)u_l(x)dx \\ &=\frac{1}{\alpha_l}\sum_{i=0}^{N} w_i\phi(x_i)u_l(x_i) . \end{aligned} \tag{3}$$

The approximate function $\phi_N(x)$ can now be represented by the exact functional values at the collocation points, namely,

$$\phi_N(x)=\sum_{i=0}^{N} g_i(x)\phi(x_i) , \tag{4}$$

where $g_i(x)$ is the cardinal function given by

$$g_i(x)=w_i\sum_{l=0}^{N} u_l(x_i)u_l(x)/\alpha_l \tag{5}$$

and possesses the unique property

$$g_i(x_j)=\delta_{ij} . \tag{6}$$

Let us first consider, for simplicity, the one-dimensional (1D) eigenvalue problem

$$\hat{H}\phi(x)=E\phi(x) , \tag{7}$$

where

$$\hat{H}=\hat{p}^2/2m+V(x) . \tag{8}$$

Under the polynomial approximation, Eq. (1), and imposing the boundary condition $\phi(x_0)=\phi(x_N)=0$, the eigenvalue problem becomes

$$\sum_{j=1}^{N-1}[\hat{H}g_j(x)-Eg_j(x)]\phi(x_j)=0 , \tag{9}$$

where the differentiation $\hat{H}g_j(x)$ can be performed exactly. One of the key points of the pseudospectral method is to require Eq. (9) to be satisfied exactly at those collocation points. This leads to the $(N-1)\times(N-1)$ matrix form eigenvalue problem

$$\hat{H}\psi=E\psi , \tag{10}$$

with

$$H_{ij}=\hat{H}g_j(x)|_{x=x_i} , \tag{11}$$

$$\psi=(\phi(x_1),\ldots,\phi(x_{N-1}))^T . \tag{12}$$

The solution of Eq. (10) provides both the bound-state energies and the values of the wave functions *directly* at the mesh points. Further, the potential-energy matrix is always *diagonal* and the kinetic-energy matrix elements are of simple analytical forms. Thus, for the 1D Hamiltonian, Eq. (8), we have

$$H_{ij}=\frac{1}{2m}(D_2)_{ij}+V(x_i)\delta_{ij} , \tag{13}$$

where

$$(D_2)_{ij}=g_j''(x)|_{x=x_i} . \tag{14}$$

We give below the analytic forms of $g_j(x)$ and $(D_2)_{ij}$ for the important case that $u_l(x)=P_l(x)=$Legendre polynomial. As will be shown later in Sec. II C, the Legendre pseudospectral method, with appropriate mapping to remove the singularity, can be efficiently and accurately applied to atomic processes with Coulomb potential—a subject of primary interest in this paper. The cardinal functions $g_j(x)$ and $(D_2)_{ij}$ are given by

$$g_j(x)=-\frac{1}{\alpha_N P_N(x_j)}\frac{(1-x^2)P_N'(x)}{x-x_j} \tag{15}$$

and

$$\begin{aligned}(D_2)_{jj}&=g_j''(x)|_{x=x_j}=-\frac{N(N+1)}{3(1-x_j)^2}, \quad 1\le j\le N-1 ,\\ (D_2)_{ij}&=g_j''(x)|_{x=x_i}=-\frac{2}{(x_i-x_j)^2} ,\\ &\qquad 1\le i,\ j\le N-1,\ i\ne j ,\end{aligned} \tag{16}$$

where x_j's are the roots of $P_N'(x)$ $(j=1,2,\ldots,N-1)$ and $\alpha_N=N(N+1)$.

B. Resonance-state complex eigenvalue problems

The pseudospectral method described above for bound-state eigenvalue problems can be extended to the resonance-state complex eigenvalue problems by means of the use of the complex-scaling transformation [19]. Consider again for simplicity the 1D system, Eq. (8). Under the complex-scaling transformation $x\to xe^{i\theta}$, the Schrödinger equation becomes ($\hbar=1$)

$$\left[-\frac{1}{2m}e^{-i2\theta}\frac{d^2}{dx^2}+V(xe^{i\theta})\right]\psi=E\psi , \tag{17}$$

where E denotes the complex energy of the resonance states. Pseudospectral discretization of this equation is straightforward, yielding an $(N-1)\times(N-1)$ complex eigenvalue problem. The non-Hermitian Hamiltonian matrix elements are written by

$$H_{ij}(\theta)=-e^{-i2\theta}(D_2)_{ij}/2m+V(x_ie^{i\theta})\delta_{ij} , \tag{18}$$

where x_i are the collocation points (not necessarily evenly spaced) corresponding to the particular choice of polynomials used in the pseudospectral method. The complex-scaling pseudospectral method has been shown to be simpler to implement and computationally more efficient than the traditional complex-scaling variational methods using the basis-set expansion [18]. The primary attractive features of the complex-scaling pseudospectral method are (i) no computation of potential matrix elements is required and the kinetic matrix elements have simple analytic forms, (ii) the eigenvectors provide directly the values of wave functions at the collocation points, (iii) no boundary conditions need to be imposed and (iv) work for both low-lying and highly excited states.

C. Generalized pseudospectral method with mapping for Coulomb problems

For atomic structure calculations involving the Coulomb potential, one typical problem with the grid methods is the singularity at $r=0$ and the long-range nature of the potential. Generally, one truncates the semi-infinite domain into finite domain $[r_{\min},r_{\max}]$ to avoid the problems of both the singularity at the origin and the infinite domain. For this purpose, $r_{\min}$ must be chosen to be sufficiently small and $r_{\max}$ sufficiently large. This results in the need of a large number of grid points, in addition to possible truncation errors. To overcome this problem, we can map the semi-infinite domain $[0,\infty]$ into the finite domain $[-1,1]$ using the mapping $r=f(x)$, and then the Legendre or Chebyshev pseudopotential technique. In this paper we shall use the algebraic mapping

$$r=f(x)=L\frac{1+x}{1-x} , \tag{19}$$

where L is a mapping parameter. Note that this mapping removes the singularity at $r=0$. Generally the introduction of nonlinear mapping can lead to either an asymmetric or a generalized eivenvalue problem [16]. Such undesirable features may be overcome by the following symmetrization procedure which has been recently intro-

duced [18]. Consider the radial Schrödinger equation, for example,

$$\hat{H}_0\psi(r)=E\psi(r) ,$$

where

$$\hat{H}_0=-\frac{1}{2m}\frac{d^2}{dr^2}+V_0(r) ,$$

and $V_0(r)$ contains the Coulomb potential. Introducing the mapping $r=f(x)$ in Eq. (19) and defining

$$\phi(x)=\sqrt{f'(x)}\psi[f(x)] ,$$

we find the transformed Hamiltonian has the following form:

$$\hat{H}_0(x)=-\frac{1}{2m}\frac{1}{f'(x)}\frac{d^2}{dx^2}\frac{1}{f'(x)}+V_0(r=f(x)) . \tag{20}$$

We see that the kinetic-energy operator is now symmetrized, leading to a symmetric eigenvalue problem.

D. Complex-scaling generalized pseudospectral method for the determination of complex quasienergies associated with multiphoton ionization processes

Corresponding to the periodically time-dependent Hamiltonian ($\hbar=1$)

$$\hat{H}(\mathbf{r},t)=-\frac{1}{2m}\nabla^2+V(\mathbf{r})+eFz\cos\omega t , \tag{21}$$

describing the interaction of one-electron atoms with a monochromatic, linearly polarized, coherent laser field of frequency ω and peak field strength F, an equivalent time-independent infinite-dimensional Hamiltonian $\hat{H}_F(\mathbf{r})$ may be obtained by the extension of the semiclassical Floquet Hamiltonian method [11,12]. The Floquet Hamiltonian $\hat{H}_F(\mathbf{r})$ has no discrete spectrum. Writing the time-evolution operator as

$$\exp(-i\hat{H}_F t)=\frac{1}{2\pi i}\int_c dz\frac{\exp(-izt)}{z-\hat{H}_F} \tag{22}$$

gives the usual result that the time dependence is dominated by poles of the resolvent $(z-\hat{H}_F)^{-1}$ near the real axis but on higher Riemann sheets, and that the complex energies of the poles are related to positions and widths $(E_R,-\Gamma/2)$ of the shifted and broadened complex quasienergy states. These complex poles may be obtained directly from the analytically continued Floquet Hamiltonian $H_F(\alpha)$ obtained by the complex-scaling transformation $\mathbf{r}\rightarrow\mathbf{r}e^{i\alpha}$. This transformation effects an analytical continuation of $(z-\hat{H}_F)^{-1}$ into the lower half-plane on an appropriate higher Riemann sheet, allowing the complex quasienergies to be determined by solution of a non-Hermitian eigenproblem. This formalism, known as the non-Hermitian Floquet Hamiltonian method [11], is usually implemented by means of the L^2 basis-set expansion and variational principle. It has been applied successfully to a number of atomic and molecular multiphoton ionization and dissociation processes in intense laser fields in the past decade [12].

The complex-scaling generalized pseudospectral method introduced earlier in this paper can be applied directly to the discretization and solution of the non-Hermitian Floquet Hamiltonian $\hat{H}_F(\mathbf{r}^{i\alpha})$. The computational advantages of this new pseudospectral discretization technique will be demonstrated.

III. MODEL POTENTIAL OF H^-

In order to obtain accurate results when comparing with the experiments, we have previously introduced an angular-momentum-dependent model potential $v_l(r)$ to describe the photoelectron, that is, we treat H^- as an effective one-electron system in which the detached electron moves in the field of a perturbed hydrogen atom. The effective interaction between the detached electron and the bound electron is chosen to reproduce the binding energy of H^- [6], and the low-energy e-H(1s) singlet elastic-scattering phase shifts [7]. The following is the form of the model potential:

$$v_l(r)=-\left[1+\frac{1}{r}\right]e^{-2r}-\frac{\alpha_d}{2r^4}W_6\left[\frac{r}{r_c}\right]+u_l(r) , \tag{23}$$

where $\alpha=4.5$ a.u. is the static polarizability of the hydrogen atom in its ground states,

$$W_j(x)=1-\exp(-x^j) \tag{24}$$

is the cutoff function, and r_c is an effective hydrogen-atom radius. The last term $u_l(r)$ in (23) is an angular-momentum-dependent short-range correction of the form

$$u_l(r)=(c_0+c_1r+c_2r^2)e^{-\beta r} , \tag{25}$$

where the coefficients c_0, c_1, c_2, and β are chosen to approximate as accurately as possible the binding energy [6] and low-energy singlet phase shifts of H^- [7]. We found it is sufficient to use two different functions $u_l(r)$: one, $u_0(r)$, for states with angular momentum $l=0$, and another, $u_l(r)$, for states with $l\geq 1$. It is also necessary to use two different functions because, for example, s- and p-wave phase shifts cannot be fitted with a common potential $v(r)$. As has been investigated in paper I [5], one-phonon photoabsorption cross sections based on this model potential are in excellent agreement with earlier accurate correlated two-electron calculations [9].

In this paper we use this model potential and perform nonperturbative studies of the intensity-dependent multiphoton detachment rates of H^- as well as the threshold behavior, using the non-Hermitian Floquet formalism and the complex-scaling generalized pseudospectral discretization technique. To facilitate the complex-scaling calculation, we replace the cutoff function W_6 above by the following form:

$$W_6(y)=1-\left[1+y+\frac{y^2}{2!}+\frac{y^3}{3!}+\frac{y^4}{4!}+\frac{y^5}{5!}\right]e^{-y} , \tag{26}$$

where $y=5r/r_c$. The values of the parameters c_0, c_1, c_2, and β are given in Table I.

TABLE I. Model potential parameters for H^-.

l	r_c	c_0	c_1	c_2	β
0	4.0	4.975 092 0	−4.724 867 7	0.272 268 01	1.4
≥1	4.0	−2.191 784 3	2.135 522 0	−0.294 768 24	1.4

IV. INTENSITY-DEPENDENT MULTIPHOTON DETACHMENT RATES OF H^-: NONPERTURBATIVE COMPLEX QUASIENERGY CALCULATIONS

In this section we shall present the results of nonperturbative calculations of the intensity-dependent complex quasienergies $(E_R, -\Gamma/2)$ of H^- in the presence of monochromatic laser fields with intensity ranging from 1 to 40 GW/cm^2. The real part (E_R) of the complex quasienergy provides the ac Stark shift of the H^- ground state, whereas the imaginary part $(\Gamma/2)$ provides the multiphoton detachment rate of H^- at a given laser frequency ω and intensity I. In the following, we first demonstrate the computational advantages of the generalized pseudospectral method.

A. Numerical test: Generalized Legendre pseudospectral discretization versus basis-set expansion and finite difference

As an example of the usefulness of the complex-scaling generalized pseudospectral method, we give in Table II the comparison of several calculations of the resonance energies of the model problem of the tunneling in the anharmonic oscillator $V(x)=x^2/4-\lambda x^3$. The methods considered are (1) CSB, complex-scaling (harmonic oscillator) basis-set expansion [20]; (2) CSFD, complex-scaling finite difference [21], and (3) CSLPS, complex-scaling Legendre pseudospectral discretization [18]. The number of grid points (N_g) or the number of basis-set functions (N_b) used are indicated. Note that all the decimal places shown in the table for CSLPS are converged with respect to the rotational angle α and to N_g or N_b. Note that the pseudospectral method (CSLPS) not only is computationally simpler and faster, but can achieve accuracy comparable to (or even higher than) that of the basis-set expansion (CSB) method. Even in this simple model problem, the CSLPS method is about four times faster than the CSB method. The pseudospectral method also appears to be more accurate and far more efficient than the earlier exploratory finite-difference method [21] using $N_g=4000$. The simplicity, efficiency, and accuracy of the CSLPS technique make it a highly competitive alternative to the conventional CSB method.

B. Intensity-dependent multiphoton detachment rates and ac Stark shifts of H^-

In this section we present the results of complex quasienergy $(E_R, -\Gamma/2)$ calculations of H^- via the non-Hermitian Floquet Hamiltonian formalism using the complex-scaling Legendre pseudospectral discretization technique. The structure of the Floquet Hamiltonian $\hat{H}_F(\mathbf{r})$ for H^- is the same as that of atomic hydrogen [11], as we treat H^- by an effective one-electron model potential. We focus our calculations in the laser frequency range 0.20–0.42 eV and laser intensity from 1 to 40 GW/cm^2. The laser frequency range covers both two- and three-photon dominant detachment processes. The number of Legendre grid points used (N_g) is typically 31–51 points, and the number of partial waves used ranges from 7 to 15, depending upon laser intensity and frequency. A sufficient number of Floquet blocks (5 to 13) is used to ensure the convergence of the complex quasienergy. Since H^- has only one bound state, the inverse iteration procedure [11] is particularly useful and effective and is adopted here. For the strongest intensity (40 GW/cm^2) considered, the dimension of the Floquet matrix is about 10 000×10 000. The computer time used for each calculation depends upon the dimensionality of the Floquet matrix (N_F), ranging from about 14 sec $(N_F=1600)$ to about 400 sec $(N_F=10\,000)$ for a CRAY 2 computer. This is several orders of magnitude faster than that using the basis-set expansion and the diagonalization of the whole non-Hermitian Floquet matrix.

Figures 1(a) and 1(b) show, respectively, the energies $(E_R$'s) and the multiphoton detachment rates (Γ's) of H^- for laser intensity $I=4$, 8, 12, 16, and 20 GW/cm^2 and laser frequency from $\omega=0.20$ to 0.42 eV. Figures 2(a)

TABLE II. Complex resonance energies $(E, -\frac{1}{2}\Gamma)$ for the anharmonic oscillator $V(x)=0.25x^2-0.034x^3$.

n	CSB ($n_b=40$)		CSLPS ($n_g=40$)		CSFD ($n_g=4000$)	
1	0.485 679 37	−0.000 002 866 98i	0.485 679 371 77	−0.000 002 866 98i	0.485 678 6	−0.000 003 0i
2	1.391 574 8	−0.001 341 93i	1.391 574 841 1	−0.001 341 934 0i	1.391 572	−0.001 342 5i
3	2.132 135 6	−0.068 762 6i	2.132 135 56	−0.068 762 61i	2.132 13	−0.068 762 i
4	2.817 874	−0.363 974 i	2.817 874 15	−0.363 973 68i	2.817 86	−0.363 967 i
5	3.586 675	−0.777 257 i	3.586 674 7	−0.777 256 8i	3.586 65	−0.777 24i

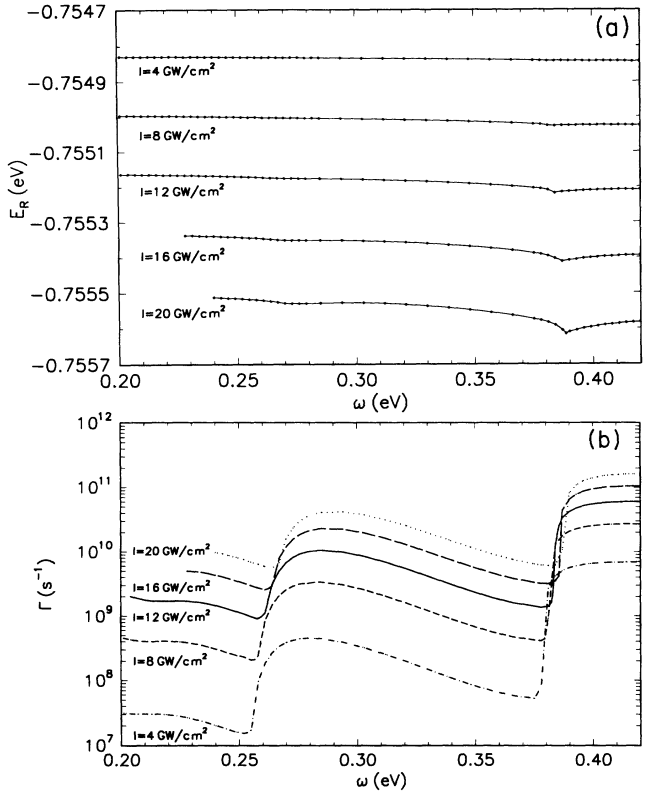

FIG. 1. The frequency- and intensity-dependent complex quasienergies $(E_R, -\Gamma/2)$ of H^- for $I=4$, 8, 12, 16, and 20 GW/cm^2 and $\omega=0.20$–0.42 eV: (a) E_R (real energies), showing the ac Stark shifts of the H^- ground state, and (b) Γ (imaginary energies), showing the multiphonon detachment rates.

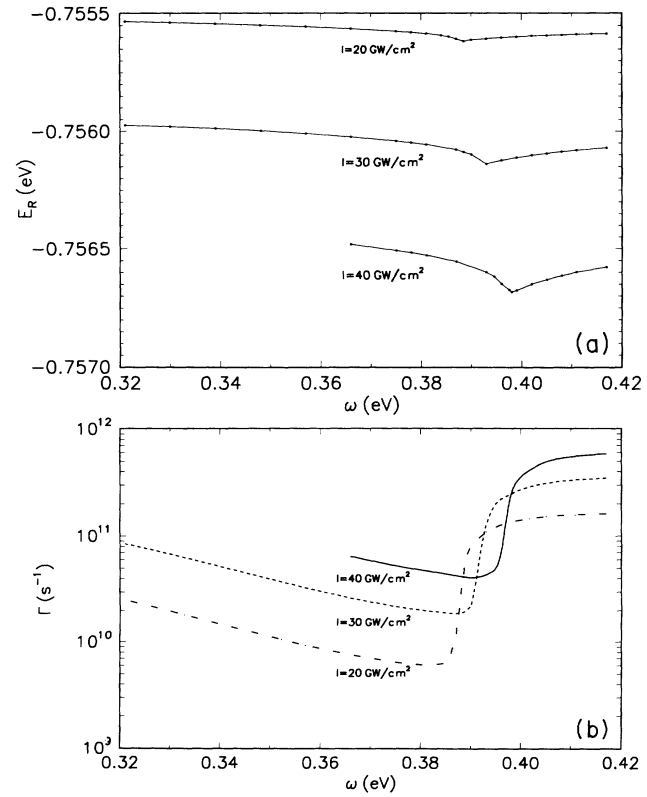

FIG. 2. Same as Fig. 1 except for higher laser intensities $I=20$, 30, and 40 GW/cm^2.

and 2(b) show the same complex quasienergies for higher laser intensity $I=20$, 30, and 40 GW/cm^2. Several distinct behaviors are noticed.

(i) The energies of the H^- ground state show significant intensity-dependent ac Stark shifts. The larger the laser intensity, the larger the ac Stark shift. The energies of the H^- ground state (at a given laser intensity) generally show smooth dependence on the laser frequency ω, except near the onset of multiphoton ionization thresholds where E_R's show dips. The positions of the dips are blueshifted and the dips are more pronounced as the laser intensity increases.

(ii) The multiphonon detachment rates (Γ) are strongly intensity dependent. For each laser intensity, the photodetachment rates show rapid change with photon frequency ω near the onset of each multiphoton ionization threshold. The lower the laser intensity, the sharper the threshold behavior. Similar to the behavior of E_R, the positions of the photodetachment threshold jumps are blueshifted as the laser intensity increases.

V. AVERAGED MULTIPHOTON DETACHMENT RATES: COMPARISON OF THEORETICAL AND EXPERIMENTAL RESULTS

In Sec. IV B we present the multiphoton detachment rates of H^- driven by monochromatic laser fields. To compare with the experimental measurement [3], we perform the following simulations of intensity-averaged multiphoton detachment rates. We simulate the experiment with a uniform H^- beam (diameter 3 mm) and a Gaussian distribution of laser intensity in space:

$$I(\rho,z)=I_0\left[\frac{W_0}{W(z)}\right]^2 e^{-2\rho^2/w^2(z)} . \tag{27}$$

I_0 is the laser peak intensity in the atom frame at the spot center ($\rho=z=0$), $W(z)$ is the spot size given by

$$W(z)=W_0(1+z^2/z_R^2)^{1/2} , \tag{28}$$

where W_0 ($=110$ μm) is the waist of the focus beam, $z_R=\pi W_0^2/\lambda$ is the associated Rayleigh range, $\lambda=10.6$ μm is the laser frequency in the laboratory frame, and z is the distance from the waist. The laser pulse used in the experiment [3] is linearly polarized and temporarily smooth and had a duration of 136 ns full width at half maximum (FWHM), and a 1-μs-long tail. Because of the long duration of the laser pulse, it is a good approximation to treat it as a monochromatic laser field.

It is useful to recall the experimental setup for the H^- experiment [3]. The 800-MeV H^- target ions travel at a speed $\simeq 2.53\times10^8$ m/s, corresponding to $\beta=v/c=0.842$ and $\gamma=1.85$, where β and γ are the usual relativistic parameters. The photon energy in the laboratory frame ($E_{\rm lab}$) was Doppler shifted to $E_{\rm c.m}$ in the center of mass (c.m.) (or, equivalently, the atom frame of the H^- ion) according to

$$E_{\rm c.m.}=\gamma(1+\beta\cos\alpha)E_{\rm lab} , \tag{29}$$

where α is the angle of intersection ($\alpha=0$ when head on) of the H^- and laser beams. The laser intensity in the

c.m. frame ($I_{c.m.}$) transforms from the laboratory value I_{lab} according to

$$I_{c.m.}=\gamma^2(1+\beta\cos\alpha)^2 I_{lab} \ . \tag{30}$$

In the Los Alamos experiment [3], the laboratory laser wavelength is fixed at $\lambda_{lab}=10.6\ \mu m$. By adjusting the intersection angle α, one can generate different laser wavelengths in the atom frame via Eq. (29). Further, according to Eqs. (29) and (30),

$$I_{c.m.}/I_{lab}=(\omega_{c.m.}/\omega_{lab})^2 \ , \tag{31}$$

where $\omega_{c.m.}$ is the laser frequency in the atom frame and $\omega_{lab}=2\pi c/\lambda_{lab}$. Equation (31) shows that for different $\omega_{c.m.}$, the H^- ions are exposed to different laser peak intensities $I_{c.m.}$; even the laboratory peak intensity I_{lab} is fixed. Further, the larger $\omega_{c.m.}$ is, the larger the laser peak intensity $I_{c.m.}$ that needs to be considered.

To perform the averaged multiphoton detachment rates, we use the expression

$$\bar{\Gamma}(\omega_{c.m.})=\int_0^{I_{peak}} W(I)\Gamma(\omega_{c.m.},I)dI \ , \tag{32}$$

where I is the laser intensity in the c.m. frame, $I_{peak}=I_{c.m.}$ is the peak intensity in the c.m. frame given in Eq. (30), and $W(I)$ is a weighting factor. In principle, $W(I)$ depends also upon $\omega_{c.m.}$, since for different $\omega_{c.m.}$, I_{peak} is different. Figure 3 shows a typical example of $W(I)$ for the case of $\omega_{c.m.}=0.39$ eV. In performing the average in Eq. (32), $\Gamma(\omega_{c.m.},I)$ are obtained from the complex quasienergy calculations for given values of I and $\omega_{c.m.}$.

We present in Fig. 4 the averaged multiphoton detachment rates determined from the above-mentioned simulation procedure corresponding to the case of $I_{lab}=4$ GW/cm^2 and $\lambda_{lab}=10.6\ \mu m$. Also shown in Fig. 4 are the experimental data [3]. The overall agreement appears quite satisfactory, well within the estimated experimental uncertainty of a factor of 5. Note that, in our simulation, there are no adjustable parameters and the fact that the absolute photodetachment rates of experimental and theoretical investigations are on top of each other is rather encouraging. The theoretical prediction of the onset of two- and three-photon thresholds are also in good accord with the experimental curve, although the theoretical curve tends to be slightly sharper at thresholds. The small discrepancy may be attributed to the difficulty in the "exact" simulation of the experimental conditions. We have previously also performed a simulation of the averaged multiphoton detachment rates using the generalized cross sections from perturbative calculations [5]. The results there were less satisfactory as the predicted onset of n-photon thresholds is much sharper than the experimental data and the current results. Further, the perturbative simulation contains a free parameter in the laser profile to fit the experimental data. Our present study indicates that nonperturbative treatment is required and capable of describing satisfactorily the process of multiphoton detachment of H^- in the Los Alamos experiments [3].

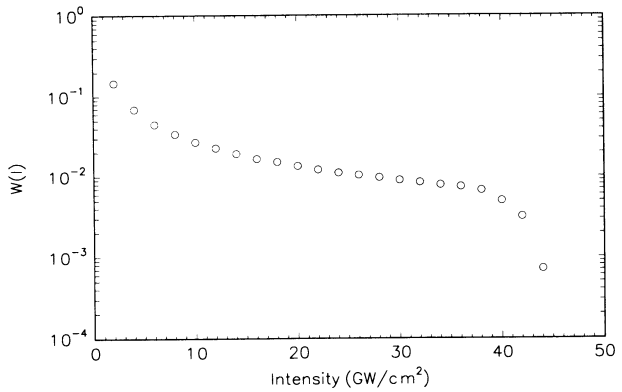

FIG. 3. A representative example of the weighting factor $W(I)$ versus laser intensity I (corresponding to $\omega_{c.m.}=0.390$ eV).

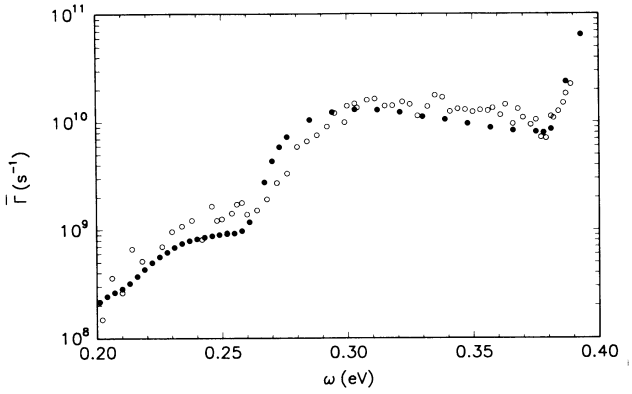

FIG. 4. Comparison of the intensity-averaged photodetachment rates for the case of $I_{lab}=4$ GW/cm^2: ●, theoretical simulation, ○ experimental data.

VI. CONCLUSIONS

In this paper we have (i) developed a computational technique, the complex-scaling generalized pseudospectral method, for accurate and efficient solution of the complex quasienergies associated with the non-Hermitian Floquet Hamiltonian, (ii) determined detailed intensity- and frequency-dependent multiphoton detachment rates and ac Stark shifts of H^- based on an accurate one-electron model potential, and (iii) performed the intensity-averaged photodetachment rate calculations by a simulation of the experimental conditions. The results (without any free parameters) are well within the estimated experimental uncertainty, both in the absolute magnitude and in the threshold behavior.

ACKNOWLEDGMENTS

This work was partially supported by the Division of Chemical Sciences, Office of Basic Energy Sciences, of the U.S. Department of Energy. We are grateful to Dr. Howard Bryant for providing the experimental data for the comparison with the present work and to Dr. C. Y. Tang for useful discussions on the experimental conditions.

[1] C. Y. Tang, P. G. Harris, A. H. Mohagheghi, H. C. Bryant, C. R. Quick, J. B. Donahue, R. A. Reeder, S. Cohen, W. W. Smith, and J. E. Stewart, Phys. Rev. A **39**, 6068 (1989).

[2] W. W. Smith, C. Y. Tang, C. R. Quick, H. C. Bryant, P. G. Harris, A. H. Mohagheghi, J. B. Donahue, R. A. Reeder, H. Sharifian, J. E. Stewart, H. Toutounchi, S. Cohen, T. C. Altman, and D. C. Rislove, J. Opt. Soc. Am. B **8**, 17 (1991).

[3] C. Y. Tang, H. C. Bryant, P. G. Harris, A. H. Mohagheghi, R. A. Reeder, H. Sharifian, H. Tootoonchi, C. R. Quick, J. B. Donahue, S. Cohen, and W. W. Smith, Phys. Rev. Lett. **66**, 3124 (1991).

[4] For a summary of recent work and a more complete list of references in this direction, see S. Geltman, Phys. Rev. A **43**, 4930 (1991).

[5] C. Laughlin and S. I. Chu, Phys. Rev. A **48**, 4654 (1993).

[6] K. R. Lykke, K. K. Murray, and W. C. Lineberger, Phys. Rev. A **43**, 6104 (1991).

[7] C. Schwartz, Phys. Rev. **124**, 1468 (1961); A. L. Stewart, J. Phys. B **11**, 3851 (1978); M. R. H. Rudge, *ibid.* **8**, 940 (1975); J. Callaway, Phys. Lett. **65A**, 199 (1978).

[8] A. Dalgarno and J. T. Lewis, Proc. R. Soc. London, Ser. A **233**, 70 (1955).

[9] A. W. Wishart, J. Phys. B **12**, 3511 (1979); A. L. Stewart *ibid.* **11**, 3851 (1978).

[10] See, for example, C. R. Liu, B. Gao, and A. F. Starace, Phys. Rev. A **46**, 5985 (1992).

[11] S. I. Chu and W. P. Reinhardt, Phys. Rev. Lett. **39**, 1195 (1977); A. Maquet, S. I. Chu, and W. P. Reinhardt, Phys. Rev. A **27**, 2946 (1983).

[12] For reviews on non-Hermitian Floquet methods, see S. I. Chu, Adv. At. Mol. Phys. **21**, 197 (1985); Adv. Chem. Phys. **73**, 739 (1989).

[13] S. I. Chu, Chem. Phys. Lett. **167**, 155 (1990); J. Chem. Phys. **94**, 7901 (1991).

[14] G. Yao and S. I. Chu, Chem. Phys. Lett. **197**, 413 (1992); Phys. Rev. A **45**, 6735 (1992).

[15] E. Layton and S. I. Chu, Chem. Phys. Lett. **186**, 100 (1991).

[16] See, for example, J. P. Boyd, *Chebyshev and Fourier Spectral Methods* (Springer, Berlin, 1989), and references therein.

[17] C. Canuto, M. Y. Hussaini, A. Quarteroni, and T. A. Zang, *Spectral Methods in Fluid Dynamics* (Springer, Berlin, 1988), and references therein.

[18] G. Yao and S. I. Chu, Chem. Phys. Lett. **204**, 381 (1993).

[19] E. Balslev and J. M. Combes, Commun. Math. Phys. **22**, 280 (1971); A. Aguilar and J. M. Combes, Math. Phys. **22**, 265 (1971).

[20] K. K. Datta and S. I. Chu, Chem. Phys. Lett. **87**, 357 (1982).

[21] O. Atabek and R. Lefebvre, Chem. Phys. Lett. **84**, 233 (1981).